Complex structures of dense lithium: Electronic origin

V F Degtyareva

Institute of Solid State Physics of the Russian Academy of Sciences, Institutskaya Street 2, Chernogolovka, Moscow Region 142432, Russia

E-mail: degtyar@issp.ac.ru

Abstract. Lithium—the lightest alkali metal exhibits unexpected structures and electronic behavior at high pressures. Like the heavier alkali metals, Li is bcc at ambient pressure and transforms first to fcc (at 7.5 GPa). The post-fcc high-pressure form Li-cI16 (at 40–60 GPa) is similar to Na-cI16 and related to more complex structures of heavy alkalis Rb-oC52 and Cs-oC84. The other high pressure phases for Li (oC88, oC40, oC24) observed at pressures up to 130 GPa are found only in Li. The different route of Li high-pressure structures correlates with its special electronic configuration containing the only 3 electrons (at $1s$ and $2s$ levels). Crystal structures for Li are analyzed within the model of Fermi sphere–Brillouin zone interactions. Stability of post-fcc structures for Li are supported by the Hume–Rothery arguments when new diffraction plains appear close to the Fermi level producing pseudogaps near the Fermi level and decreasing the crystal energy. The filling of Brillouin–Jones zones by electron states for a given structure defines the physical properties as optical reflectivity, electrical resistivity and superconductivity. To understand the complexity of structural and physical properties of Li above 60 GPa it is necessary to assume the valence electron band overlap with the core electrons and increase the valence electron count under compression.

1. Introduction

Recent high pressure studies of the structure and properties of elements under high pressure bring considerable revision to what has been known previously (see review papers [1–3] and references therein). At normal conditions, the group-I elements of the periodic table from Li to Cs are related to the free-electron metals and adopt the body-centered cubic (bcc) structure. They transform under pressure to the face-centered cubic (fcc) structure and at significant compression to open-packed and complex structures. Li is the lightest metal containing only 3 electrons (at $1s$ and $2s$ levels) and its special electronic configuration results in a different sequence of Li high-pressure structures. For dense lithium a departure from nearly free-electron behavior and tendency to "a pairing of the ions" has been predicted by Neaton and Ashcroft [4]. The post-fcc high-pressure form Li-cI16 (at 40–60 GPa) [5] is similar to Na-cI16 and related to more complex structures of heavy alkalis Rb-oC52 and Cs-oC84. The other high pressure phases for Li (oC88, oC40, oC24) found at pressures up to 130 GPa are specific to only Li [6,7].

Physical properties of Li under compression change essentially. An increase in resistivity has been reported under dynamic and static pressure [8,9]. A remarkable increase of the superconducting temperature from 0.4 mK at ambient pressure to 14–20 K at pressures 40–70 GPa has been found [9–11]. Recently a reentrant semiconductor to metal transition was

found for Li at 80–120 GPa [12]. Unusual drop was observed in the melting temperature of lithium below 200 K at 40 GPa [6].

For heavier alkali metals all changes in structure and properties are usually accounted by the conversion of valence electrons from s to d states [13], with the upper empty d-band moving downward on compression and overlapping with the s-band. For lithium a pressure driven s–p transition has been suggested [5]. It is assumed that at high degrees of volume compression the valence electrons are localized in the interstitial sites forming a "pseudebinary" ionic or "electride" compound [14].

In this paper possible causes are investigated that contribute to the formation of the complex crystal structures in lithium under pressure and compare these with structures of heavier alkalis. The electronic energy contribution is suggested as a cause for the formation of complex crystal structures and changes the physical properties.

2. Theoretical background and method of analysis

The crystal structure of metallic phases is defined by two main energy contributions: electrostatic (Ewald) energy and the electron band structure term. The latter usually favours the formation of superlattices and distorted structures. The energy of valence electrons is decreased due to a formation of Brillouin planes with a wave vector q near the Fermi level k_F and opening of the energy pseudogap on these planes if $q_{hkl} \approx 2k_F$ [15]. Within a nearly free-electron model the Fermi sphere radius is defined as $k_F = (3\pi^2 z/V)^{1/3}$, where z is the number of valence electrons per atom and V is the atomic volume. This effect, known as the Hume–Rothery mechanism (or electron concentration rule), was applied to account for the formation and stability of the intermetallic phases in binary simple metal systems like Cu–Zn, and then extended and widely used to explain the stability of complex phases in various systems, from elemental metals to intermetallics [16–19].

The stability of high-pressure phases in lithium are analyzed using a computer program BRIZ [20] that has been recently developed to construct Brillouin zones or extended Brillouin–Jones zones (BZ) and to inscribe a Fermi sphere (FS) with the free-electron radius k_F. The resulting BZ polyhedron consists of numerous planes with relatively strong diffraction factor and accommodates well the FS. The volumes of BZ's and FS's can be calculated within this program. The BZ filling by the electron states V_{FS}/V_{BZ} is estimated by the program, which is important for the understanding of electronic properties and stability of the given phase. For a classical Hume–Rothery phase Cu_5Zn_8, the BZ filling by electron states is equal to 93%, and is around this value for many other phases stabilized by the Hume–Rothery mechanism.

Diffraction patterns of these phases have a group of strong reflections with their q_{hkl} lying near $2k_F$ and the BZ planes corresponding to these q_{hkl} form a polyhedron that is very close to the FS. The FS would intersect the BZ planes if its radius, k_F, is slightly larger then $q_{hkl}/2$, and the program BRIZ can visualize this intersection. One should keep in mind that in reality the FS would usually be deformed due to the BZ–FS interaction and partially involved inside the BZ. The ratio $2k_F/q_{hkl}$, called a "truncation" factor, is an important characteristic for a phase stabilized due to a Hume–Rothery mechanism. For Hume–Rothery phases such as Cu_5Zn_8, this factor is equal 1.015, and it can reach up to 1.05–1.07 in some other phases. Thus, with the BRIZ program one can obtain the qualitative picture and some quantitative characteristics on how a structure matches the criteria of the Hume–Rothery mechanism.

3. Results and discussion

Several high-pressure structures of lithium are analyzed to reveal effects of the Hume–Rothery mechanism on occurrence of structural complexity. The Li-cI16 structure is considered as a distortion and superlattice of the bcc structure. The Li phase with the orthorhombic 24-atom cell is compared with one of the phases in Na (structural data are presented in table 1).

Table 1. Structure parameters of Li phases as given in the literature: Fermi sphere radius k_F, the ratio of $2k_F$ to Brillouin zone vectors $(2k_F/q_{hkl})$ and the filling degree of Brillouin zones by electron states V_{FS}/V_{BZ} are calculated by the program BRIZ [20].

| Phase	Li-bcc	Li-cI16	Li-oP24	Na-oP8
		Structural data		
Space group	$Im\bar{3}m$	$I\bar{4}3d$	$Pbca$	$Pnma$
P, T conditions	Ambient conditions	$P = 39$ GPa	$P = 115$ GPa	$P = 119$ GPa
Lattice parameters (Å)	$a = 3.5091$	$a = 5.2716$	$a = 4.213$ $b = 4.205$ $c = 7.482$	$a = 4.765$ $b = 3.020$ $c = 5.251$
Atomic volume (Å^3)	21.605	9.156	5.52	9.45
V/V_0	1	0.424	0.255	0.239
Reference	[1]	[5]	[6,7]	[21]
		FS–BZ data from the BRIZ program		
z (number of valence electrons per atom)	1	1	2	2
k_F (Å^{-1})	1.110	1.479	2.205	1.844
Total number of BZ planes	12	24	50	30
$k_F/(1/2q_{hkl})$ max	0.877	1.013	1.055	1.074
$k_F/(1/2q_{hkl})$ min			0.875	0.886
Filling of BZ with electron states V_{FS}/V_{BZ}	0.5	0.89	0.932	0.932

3.1. Li-cI16 structure as the Hume–Rothery phase

The post-fcc phase of Li at pressures ~ 39 GPa has a rhombohedral cell and is specific to lithium [5]. The structure Li-hR1 is a distortion of the fcc structure, with the compression along the body-diagonal and an increase of the rhombohedral angle from $60°$ to $62.87°$ (c/a decreases from 2.45 for fcc to $c/a = 2.296$ for Li-hR1 at 39.8 GPa). At the fcc–hR1 transition the (111) fcc plains divided into two sets: one set (101) is approaching closer to the Fermi sphere and another set (003) is moving away. A closer contact of (101) plains to the FS leads to the gain in the band structure energy. The first complex phase of lithium was found at pressures above 40 GPa with the cI16 structure [5]. Li-cI16 is $2 \times 2 \times 2$ superlattice of bcc with slight shifts of atoms resulting in the formation of new (211) planes just in contact with the FS. The new BZ is $\sim 90\%$ filled by the electron states, satisfying the Hume–Rothery rules [2,16].

3.2. Valence electron count in Li above 60 GPa

The Li structure found at pressures above 95 GPa was identified as an orthorhombic cell containing 24 atoms [6,7]. Several space groups were suggested for this structure [7]. For our analysis the oP24 type structure was selected with the experimentally found lattice parameters [6] as given in table 1.

The Li-oP24 structure can be considered in relation to the oP8 structure found for heavier alkali metals Na and K [21,22]. The diffraction patterns of Li-oP24 and Na-oP8 in figure 2 are characterized by the appearance of a group of reflections close to $2k_F$ and hence by a formation of several Brillouin zone planes near the FS. Configurations of BZ's are similar for both phases with some additional planes for Li-oP24 due to formation of superlattice along one axis. The
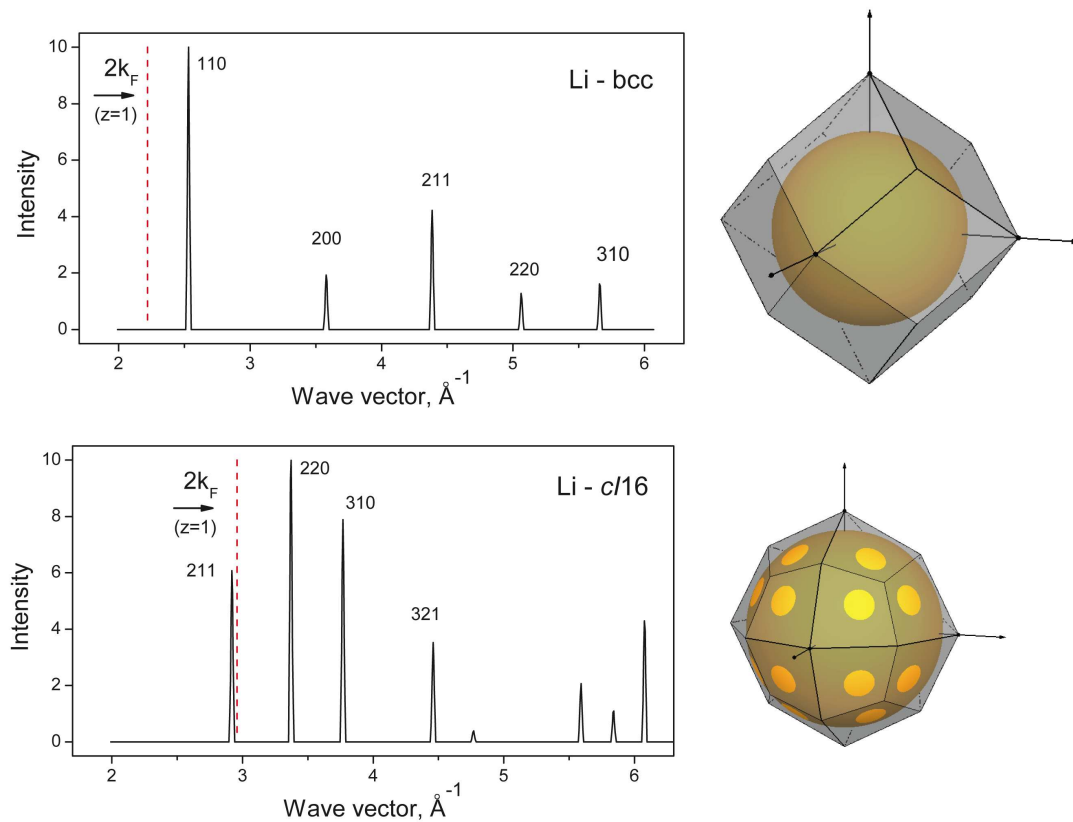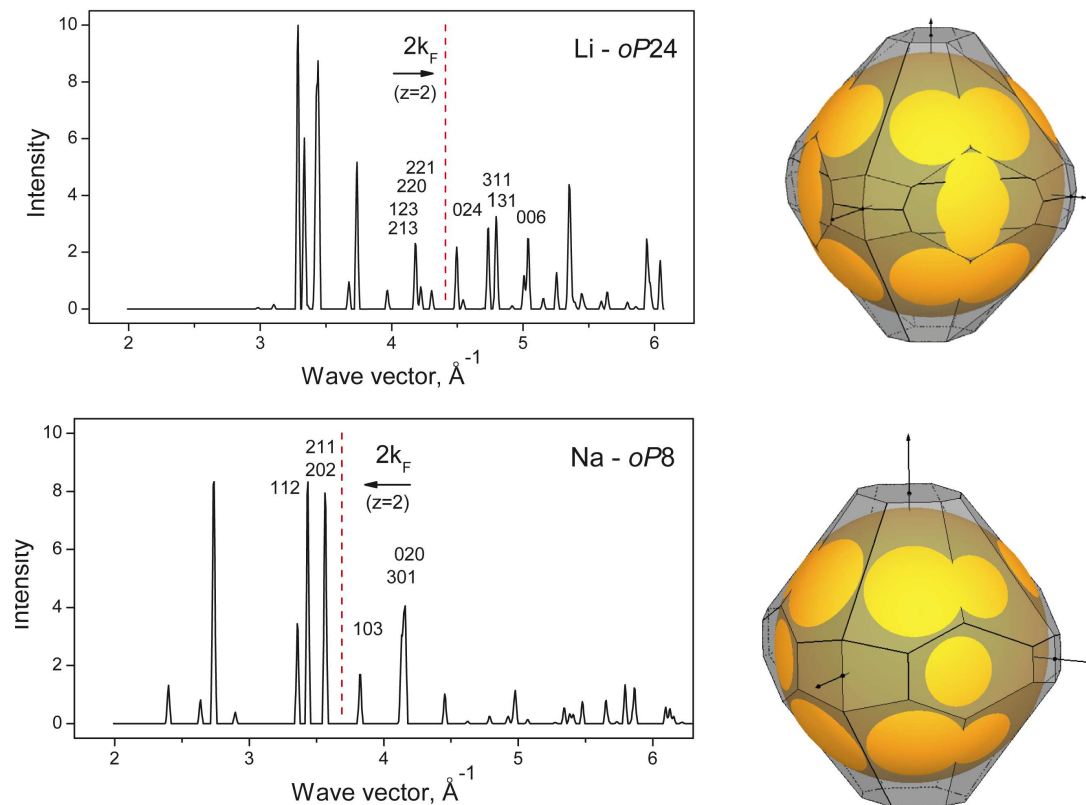
Figure 1. Calculated diffraction patterns (left) and corresponding Brillouin zones with the inscribed FS (right). In the top panel—for Li-bcc, $cI2$ and in the bottom panel—for Li-$cI16$ with structural parameters given in table 1. The position of $2k_F$ for given z and the hkl indices are indicated on the diffraction patterns. Brillouin zones are shown in common view with a^* pointing forward and c^* pointing up.

prototype hexagonal cell is NiAs-$hP4$ type and its distortion to $oP8$-type was analyzed in the case of Na [16]. Cell parameters a, b, c of the orthorhombic phases are related to the hexagonal cell parameters a_h, c_h as follows:

$$c_h,\ a_h,\ a_h\sqrt{3}\ \text{for Na-}oP8\ \text{and}\ a_h\sqrt{3},\ c_h,\ 3a_h\ \text{for Li-}oP24.$$

Valence electron number $z = 2$ is assumed for Li-$oP24$ as in Na-$oP8$ and AuGa-$oP8$ phases [16]. The double ionic radius for coordination number CN = 8–11 for lithium was estimated by Shannon [23]. These values are 0.92 Å $\times 2 = 1.84$ Å and 1.1 Å $\times 2 = 2.2$ Å for CN equal 8 and 11, respectively. The interatomic distances for Li-$oP24$ structure have close or even less values implying the core–valence band overlap at such compression. For structure stability it is necessary to assume core ionization: an overlap of the core electrons with the valence electron band of sp type. Resulting valence electron count should be increased and univalent alkali metal Li turns into a divalent metal. Similar analysis has been performed for Na and it has been suggested to become a divalent metal in the $oP8$ phase [20].

For post-$cI16$ phases of Li with compression $V/V_0 < 0.35$ an overlap of valence and core electron levels was suggested with an increase of effective valence electron number. This allows an understanding of the semiconducting properties of $oC88$ and $oC40$ phases as filling of BZ

Figure 2. Calculated diffraction patterns (left) and corresponding Brillouin zones with the inscribed FS (right). In the top panel–for Li-$oP24$ and in the bottom panel–for Na-$oP8$ with structural parameters given in table 1. The position of $2k_F$ for given z and the hkl indices of the principal planes are indicated on the diffraction patterns. Brillouin zones are shown for Li-$oP24$ in common view and for Na-$oP8$ in the view with c^* pointing forward and b^* pointing up.

by electron states and the returning $oP24$ to metal in the $oP24$ phase. The BZ filling by electron states for Li-$oP24$ is $\sim 93\%$ (see table 1)—the typical value for the metallic brass-type phases [16].

For the heavier alkali metals Na and K along with $oP8$ phases incommensurate host–guest structures were observed [1,3]. These structures were discussed in [24] with the suggestion of an overlap of the valence band and the upper core electrons resulting in the higher valence electron counts. For the heaviest alkalis K, Rb and Cs a complex structure $oC16$ has been found, the same as for group-IV (Si, Ge) elements. These findings support an assumption for heavy alkalis an increase of valence electron counts to four due to core ionization [17].

4. Summary
The formation of the Li-$cI16$ structure at pressures around 40 GPa is explained with the increase of the Hume–Rothery mechanism under compression. The ambient pressure bcc structure undergoes distortions and superlattice formation leading to the creation of a new 24-planes Brillouin zone that accommodates the Fermi sphere with the $\sim 90\%$ filling by electron states. It is considered a close structural relationship of the alkali metal structures Li-$oP24$, Na-$oP8$ and K-$oP8$ with the binary alloy phase AuGa-$oP8$. The latter phase is related to the family

of the Hume–Rothery phases that is stabilized by the Fermi sphere–Brillouin zone interaction where a decrease in the electronic band structure energy occurs due to the contact of the Fermi sphere and Brillouin zone planes. An important characteristic is degree of Brillouin zones filling by electron states which depends on the count of valence electrons per atom and the number of atoms in the cell. From similar considerations for alkali elements a necessary condition for structural stability emerges in which the valence electron sp band overlaps with the core electrons and the valence electron count increases under compression. Consideration of the core–valence electron band transfer may promote a better understanding of non-traditional behavior of alkali elements under significant compression. Changes of physical properties of Li under pressure can be accounted for with the increase of valence electron energy contribution and moreover with the overlap of core and valence electron bands. Within applied model main tendencies can be understood for structural and physical transformations in elements under strong compression.

Acknowledgments

References

[1] McMahon M I and Nelmes R J 2006 *Chem. Soc. Rev.* **35** 943–63
[2] Degtyareva V F 2006 *Phys. Usp.* **49** 369–88
[3] Degtyareva O 2010 *High Press. Res.* **30** 343–71
[4] Neaton J B and Ashcroft N W 1999 *Nature* **400** 141–144
[5] M Hanfland K Syassen N E C and Novikov D L 2000 *Nature* **408** 174–178
[6] Guillaume C L *et al* 2011 *Nat. Phys.* **7** 211–214
[7] Marqués M *et al* 2011 *Phys. Rev. Lett.* **106** 095502
[8] Fortov V E *et al* 2001 *JETP Lett.* **74** 418–421
[9] Shimizu K *et al* 2002 *Nature* **419** 597–599
[10] Struzhkin V V *et al* 2002 *Science* **298** 1213–1215
[11] Deemyad S and Schilling J S 2003 *Phys. Rev. Lett.* **91** 167001
[12] T Matsuoka M S *et al* 2014 *Phys. Rev.* B **89** 144103
[13] Ross M and McMahan A K 1982 *Phys. Rev.* B **26** 4088–93
[14] Marqués M *et al* 2009 *Phys. Rev. Lett.* **103** 115501
[15] Jones H 1962 *The Theory of Brillouin Zones and Electron States in Crystals* (Amsterdam: North-Holland)
[16] Degtyareva V F and Degtyareva O 2009 *New J. Phys.* **11** 063037
[17] Degtyareva V F 2013 *Crystals* **3** 419–30
[18] Degtyareva V F 2014 *Solid State Sci.* **36** 62–72
[19] Degtyareva V F and Afonikova N S 2013 *J. Phys. Chem. Solids* **74** 18–24
[20] Degtyareva V F and Smirnova I S 2007 *Z. Kristallogr.* **222** 718–21
[21] Gregoryanz E *et al* 2008 *Science* **320** 1054–57
[22] Lundegaard L F *et al* 2009 *Phys. Rev.* B **80** 020101
[23] Shannon R D 1976 *Acta Cryst.* **A32** 751–67
[24] Degtyareva V F 2015 *J. Phys.: Conf. Ser.* **653** 012075